The Aerodynamic Effects of the Blade Lean on a High-Aspect-Ratio Transonic Axial Flow Rotor

Mansour Asghari *
Department of Mechanical and Aerospace Engineering,
Malek Ashtar University of Technology, Isfahan, Iran
E-mail: asghari@mut-es.ac.ir
*Corresponding author

Mohsen Agha Seyed Mirzabozorg
Department of Mechanical and Aerospace Engineering,
Malek Ashtar University of Technology, Isfahan, Iran
E-mail: mirzabozorg@mut-es.ac.ir

Mahmoud Adami
Department of Mechanical and Aerospace Engineering,
Malek Ashtar University of Technology, Isfahan, Iran
E-mail: adami@mut-es.ac.ir

Received: 23 January 2018, Revised: 12 February 2018, Accepted: 9 April 2018

Abstract: In this study, the effect of tangential blade lean on the aerodynamic characteristics of low-transonic, high-aspect-ratio axial flow compressor rotor has been investigated by using the computational fluid dynamics. The B-Spline curvature with four control points of 25%, 50%, 75% and 100% of span have been used to define the blade stacking line. Various leaned rotors have been created by rotating the circumferential position of control points and they have been simulated by Computational Fluid Dynamics (CFD). At the best state, the leaned blade improves the adiabatic efficiency and total pressure ratio of compressor about 0.55% and 0.75%, respectively. The results show that, lean angle at 100% span has most effect in the peak adiabatic efficiency rather than lean angle at other control points. Also, the results indicate that, in low-transonic, high-aspect-ratio rotor blades, the tangential change of the stacking line only causes the reduction of secondary flow, while the previous studies on high-transonic low-aspect-ratio rotor blades, such as NASA Rotor 37 and NASA Rotor 67 revealed the movement of shock wave toward the downstream and the reduction of the secondary flow.

Keywords: Adiabatic efficiency, Axial flow Compressor, CFD, High-Aspect-Ratio, Low-Transonic rotor, Tangentially leaned

Reference: Mansour Asghari, Mohsen Agha Seyed Mirzabozorg and Mahmoud Adami, “Aerodynamic Effects of the Blade Lean in a High-Aspect-Ratio Transonic Axial Flow Rotor”, Int J of Advanced Design and Manufacturing Technology, Vol. 11/No. 2, 2018, pp. 85-93.

Biographical notes: M. Asghari is currently PhD candidate in the Faculty of Mechanical Engineering, Malek Ashtar University of Technology, Isfahan, Iran. His current research focuses on Computational Fluid Mechanics and Aerodynamics. **M. Agha Seyed Mirzabozorg** received his PhD and MSc in mechanical engineering from Cranfield University, United Kingdom, in 1986 and 1981. His current research focuses on aerothermodynamics, turbomachinery and aerospace propulsion. **M. Adami** received his PhD, MSc and BSc in mechanical engineering from Kansas University, U.S.A, in 1990, 1985 and 1983 respectively. His main research interest includes fluid mechanics, thermodynamics and heat transfer.

© 2018 IAU, Majlesi Branch

1 INTRODUCTION

Today, the axial transonic compressors play an important role in the performance of advanced Turbojet engines. Using high efficiency and pressure ratio compressors, the reduction of stages causes the reduction of fuel consumption, size and weight of the engines. Leaned rotor blades are one of the science-based methods used for improving the transonic compressor efficiency. According to the related literatures and based on two sets of perpendicular axes, there are two definitions for a leaned blade:

1- Moving the blade sections perpendicular to the local chord line which in some references is called "Dihedral".
2- Moving the blade sections tangential with the rotational direction which is the most common definition and is used in this study. In some literatures, this definition was referred as Bowed, and Skewed blade.

Weingold et al. numerically and experimentally studied the effects of bowing on the high-performance compressor stator blades. He showed that, due to the generation of radial forces, the bowed stators lead to the reduction of diffusion rates in the suction surface corners. Consequently, the onset of corner separation postpones and the compressor efficiency improves [1]. Sasaki and Breugelmans experimentally investigated the effects of two stacking lines (sweep and dihedral) on a linear cascade compressor. The geometries of both stacking lines consist of a straight central section which is symmetrical with the mid-span, either on the swept or dihedral sections toward the end-walls.

They observed that, on the positive dihedral (i.e. the angle between the suction surface and the end-wall), the blade loading reduces at the end-wall and then increases at the mid-span. They also discovered that, the corner stall and the secondary flow are reduced and the positive dihedral blades are more effective than the swept blades in a wide range of incidence angles [2]. Gummer et al. numerically and experimentally studied the effects of BR710 engine compressor stators with sweep and dihedral on the performance. He revealed that, the positive dihedral causes the improvement of radial loading distribution and the development of three-dimensional end-wall boundary layer leading to the reduction of end-wall losses and the enhancement of operating range on compressor stators [3].

Gallimore et al. numerically and experimentally investigated the usage of sweep and dihedral in the axial flow of multistage compressor blading (Trent engines) and in the low-speed Deverson compressor rotor. He stated that, the positive dihedral can reduce the hub corner and tip clearance losses [4], [5]. Roy et al. studied the effects of sweep and dihedral on low-speed compressor cascades. He also investigated a straight, swept, and dihedral cascade, separately. According to his study, both of the sweep and dihedral cascades have lower end-wall losses than the straight cascade and in the positive dihedral, the span-wise pressure gradient reduces near to the mid-span region, however, the chord-wise pressure gradient enhances near to the mid-span [6]. Bergner et al. showed that, by using lean, a significant change happens in the shock pattern [7].

Fisher et al. investigated the effect of strongly bowed stator vanes on a four-stage, high-speed axial compressor with controlled diffusion airfoil (CDA) blading. His numerical and experimental results showed that, the bowed stator vanes move the flow from the near-wall regions toward the mid-span in the front parts of the vanes. This behaviour causes lower loading close to the wall at the deceleration part of the vane and reduces or eliminates the corner stall at the hub. Then, the overall static pressure, total pressure and the overall efficiency are increased due to the postponement of separation [8]. Ahn and Kim optimized the stacking line of the axial flow rotor (NASA Rotor 37) by changing it to a tangential direction (the positive lean at the hub and the negative lean at the tip) and by doing so, they improved the efficiency to 0.7% [9]. Denton and Xu investigated the effects of sweep and lean on the performance of transonic fan. They showed that, although the blade sweep or lean produces very little changes in the peak efficiency, the forward swept blade improves the stall margin significantly [10].

Oyama et al. optimized the shape of the transonic axial flow blade (NASA rotor 67) by using an evolutionary algorithm and the three-dimensional Navier-Stokes solver. By modifying the stacking line (positive lean at the hub and tip) and blade profiles, he reduces the entropy generation to 16% [11]. The experimental and numerical investigations of end-wall flow in a bowed compressor cascade have been done by Takahashi et al. [12]. He observed that, in bowed stator, the blade loading at the end-wall region is lower than the straight-stacking blade, therefore, the vortexes are less and weaker than those in the straight stator blade. Jang et al. optimized the transonic axial compressor rotor by using sweep, lean and skew stacking lines. His results reported the reduction of hub corner and tip losses. Also, in the optimized blade, the passage shock and boundary layer interferences on the blade suction surface entail the movement of separation line toward the downstream. He also discovered that, among the sweep, lean and skew blades, the skew blade (tangentially leaned) is the most effective factor for improving the adiabatic efficiency of compressor rotor [13]. Yang et al. optimized the low-pressure axial fan blade using skew. He indicated that, the total pressure

© 2018 IAU, Majlesi Branch

drop significantly reduces near the hub and shroud end-wall regions, however, the total pressure drop slightly enhances at mid-span [14]. Zhang et al. studied the effect of camber angle on flow domain in the linear bowed compressor stator with low Mach number. He found that, the bowed blade has more positive effect on the high aerofoil camber angle cascade [15].

Benini performed a multi-objective optimized design on NASA Rotor 37 and showed that, by using proper tip blade lean on the direction of rotation (negative lean), due to the modification of shock structure in blade passage, the overall efficiency can be significantly improved [16]. Benini and Biollo numerically investigated the effect of sweep and lean on the transonic axial compressor rotor (NASA Rotor 37). They showed that, the leaned blades in compressor rotor can change the shock structure and improve the adiabatic efficiency up to 1.2% (by using negative lean), however, the choking and stall mass flow rates are not obviously changed [17]. Sun et al. studied the effects of bowed stators on transonic fan in a distorted inlet. He showed that, in the distorted inlet, especially at design points, the bowed stators can significantly improve the fan performance [18].

Chen et al. experimentally studied the twisted-bowed stators in an axial transonic fan stage and concluded that, the twisted-bowed stators with larger camber angles improve the aerodynamic performances in the high-loaded transonic fan stages [19]. Razavi and Boroomand, for increasing the efficiency, operating range and pressure ratio, optimized the leaned rotor blades (NASA Rotor 67) and by doing so, the optimized leaned blade effectively causes the increase of efficiency, safe operating range and pressure ratio [20].

The reviewed literatures show that, the leaned blade causes the reduction of secondary flows and moves the leading edge shock wave toward the downstream; therefore, the performance characteristics are improved. However, the leaned blade technology implement is used only in high transient, low-aspect ratio blades. Also, according to the references, the deterministic recommendations about the proper curvature in the tangential stacking lines of rotor have been not presented.

In present study, some leaned blades in tangential directions have been investigated for better understanding of curved stacking line effects on the aerodynamic behaviour of a low-transonic, high-aspect ratio compressor rotor. For this reason, the central area of stream wise blade at 0.25%, 50%, 75% and 100% of span are considered as the control points. The stacking line is formed by connecting the control points. A large number of the geometrical models of blades are created by rotating the tangential position of these control points. All of the blades are numerically analysed by an accurate CFD model. The static test conditions are considered in the numerical simulation and by changing the back pressure, different inlet axial velocities have been reached. By using these methods, the compressor map is simulated for 11 operational points of compressor.

2 OPERATIONAL CONDITIONS AND GEOMETRY

The studied rotor is the first stage of J85's compressor and has high-aspect-ratio with the rotational speed of 16640 rpm. The standard sea level air conditions are considered as inlet conditions, P_{0_Inlet} and T_{0_Inlet}. The value of outlet static pressure of compressor (P_{0_Outlet}) is 60 kPa (near the chock condition) to 95 kPa (near the stall condition) in 11 steps.

The detailed specifications of rotor and the inlet guide vane (IGV) are presented in Table 1. The IGV includes 15 blades and their leading edge metal angle is zero. The trailing edge metal angle of IGV blades, from hub to mid-span, is zero and then, it changes to 6 degrees at the tip. The meridional view of IGV and the first stage rotor of axial compressor are shown in Fig. 1.

Table 1 Design specification of IGV and rotor

Number of IGV blades	15
Number of rotor blades	22
Rotor hub to tip radius ratio	0.392
Rotor aspect ratio	2.92
Rotor tip solidity	1.01
Rotor Tip clearance (% span)	0.646 mm (0.5)

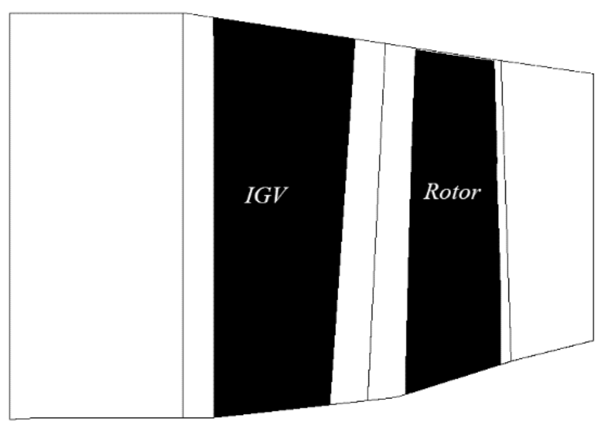

Fig. 1 Meridional view of the IGV and the first stage rotor of axial compressor.

Staking line is formed by connecting the central area of stream wise blade sections. The new geometries of the rotor are created by rotating the initial blade stacking line on the circumferential direction. As it is shown in Fig. 2, the initial stacking line of the rotor is modified by passing B-Spline from four control points in 25%,

© 2018 IAU, Majlesi Branch

50%, 75% and 100% of the height of span from the hub.

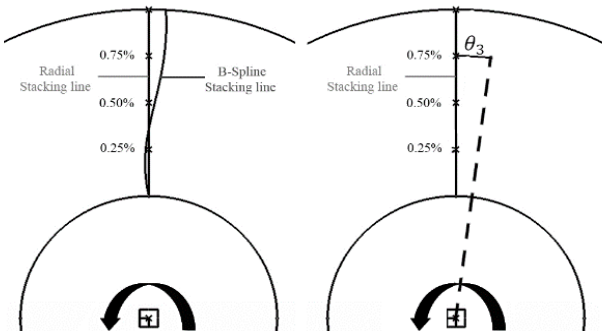

Fig. 2 Radial and B-Spline stacking line with control points.

According to Fig. 2, the angle between radial stacking line and the line connecting each control point to the center of rotor disk is called lean angle and is indicated by θ. Table 2 presents the variations of lean angle ranges in all of the control points.

Table 2 The variations of lean angle ranges in each control point

Lean angle	Variations limit (deg)
θ_1	[-0.5,0.5]
θ_2	[-1.0,1.0]
θ_3	[-2.0,2.0]
θ_4	[-3.0,3.0]

According to the values of θ_1 to θ_4, a large number of blades have been designed. However, due to the structure, weight and manufacturing limitations, just 40 designs have been selected for the numerical simulation. It should be noted that, the blade designs in which their blade length is more than 10% of radial stacking line, have been neglected.

3 METHODOLOGY

A three-dimensional commercial solving package is used for simulating the flow field. By using finite volume method, this package solves the three-dimensional Reynolds-averaged Navier–Stokes equations. Also, an algebraic multi-grid method based on Additive Correction Multi-grid strategy (ACM) has been used (Hutchinson and, Raithby [21]).

The high-resolution advection scheme has been used as a method for discretizing the finite-volume equations. The high-resolution advection scheme is a smart discretization method which uses the first-order discretization scheme in low-variable gradient regions and in order to prevent the overshoots and undershoots and maintain robustness in areas with sharp gradients, applies the second-order discretization scheme. For solving the turbulent boundary layer, SST turbulence model (Launder and Spalding [22]) with the automatic wall functions has been used. A composite grid system structured with H/J/C/L topology has been used to represent the complex configuration of the axial compressor. Approximate to the wall of IGV and the rotor blade surfaces, the grid spacing has been adopted for $y^+<1$. The computational domain, showed in Fig. 3, includes of 800,000 cells (about 300,000 for IGV and 500,000 for rotor domain).

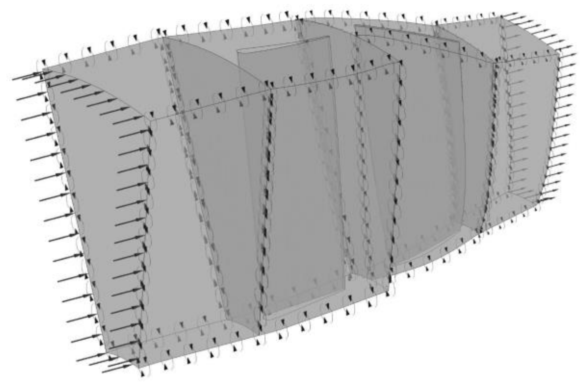

(a): IGV & Rotor domain

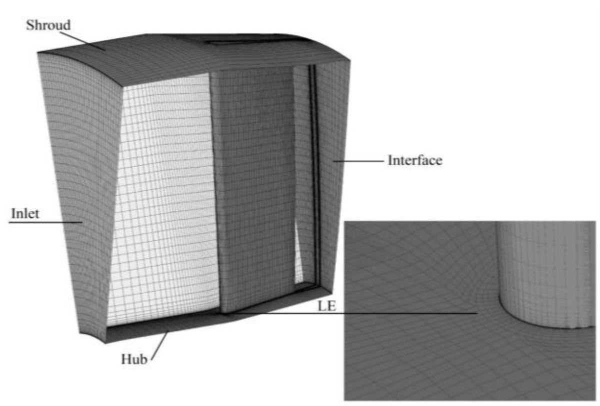

(b): IGV domain mesh

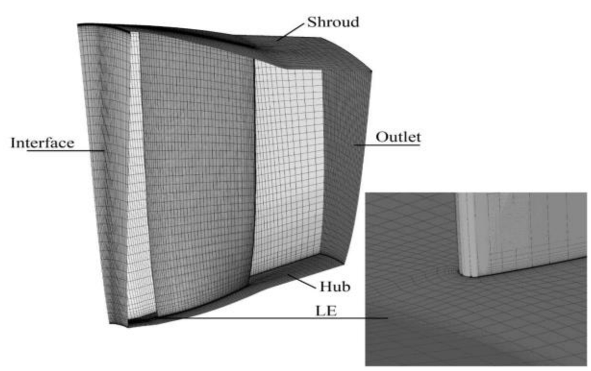

(c): Rotor domain mesh

Fig. 3 Computational domain grid of IGV and Rotor, (a): IGV & Rotor domain, (b): IGV domain meshes and (c): Rotor domain meshes.

The overall performance of different leaned blade rotors is evaluated based on the adiabatic efficiency which is defined as:

$$\eta = \left(\left(\frac{P_{0\_Outlet}}{P_{0\_Inlet}} \right)^{\frac{(\gamma-1)}{\gamma}} - 1 \right) \Big/ \left(\left(\frac{T_{0\_Outlet}}{T_{0\_Inlet}} \right) - 1 \right) \quad (1)$$

Respectively, P_{0_Outlet} and T_{0_Outlet} are the area averaged of total pressure and temperature at domain outlet.

4 VALIDATION

Experimental results of NASA Rotor 37 presented by Moore and Reid [23] have been used for validating the results of this study. The transonic axial rotor of NASA Rotor 37 consists of 36 Multiple Circular Arc (MCA). The detailed specifications of this rotor are summarized in Table 3.

Table 3 Geometry and Design specifications of NASA Rotor37

Inlet hub to tip radius ratio	0.7
Blade aspect ratio	1.19
Tip solidity	1.29
Tip clearance gap (% span)	0.356 mm (0.45)
Number of blades	36
Design pressure ratio	2.106
Design efficiency	0.877
Design mass flow rate	20.19 (kg/s)
Measured-choking mass flow rate	20.93 (kg/s)
Design wheel speed	17188.7 rpm (1800 rad/s)
Nominal tip speed	454 m/s

The computational domain is discretized to multi-blocks and then each block is meshed by a structured grid (Fig. 4). An H-type grid is used for both of the inlet and outlet blocks, while a J-grid is utilized for the passage block. Since using an SST turbulence model adopts the boundary layer mesh around the blade, so that $y^{+}<1$. The total number of cells, including tip-clearance gap, are about 430,000 cells.

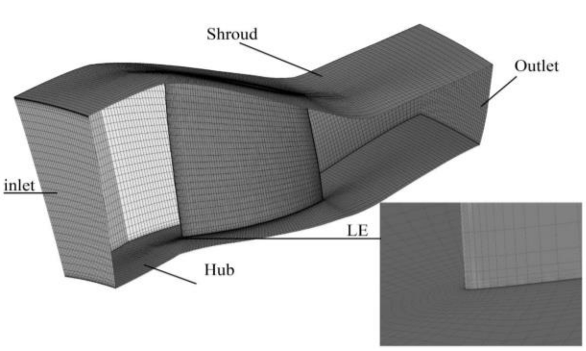

Fig. 4 Computational grid domain of NASA Rotor 37.

For the inflow boundary condition, the stagnation pressure and temperature are constant amounts, while at the outflow, the average static pressure is applied. Lateral surfaces of the flow domain are implied as a periodic boundary and the walls are considered as adiabatic. A corresponding angular velocity is applied to the domain.

The experimental and numerical rotor performance maps are presented in Fig. 5. The mass-flow rates are normalized by using the corresponding mass-flow at choking condition. The CFD model predicts the choking mass-flow at 20.95 kg/s, while the measured value is 20.93 kg/s, which shows good compatibility between the numerical and experimental results.

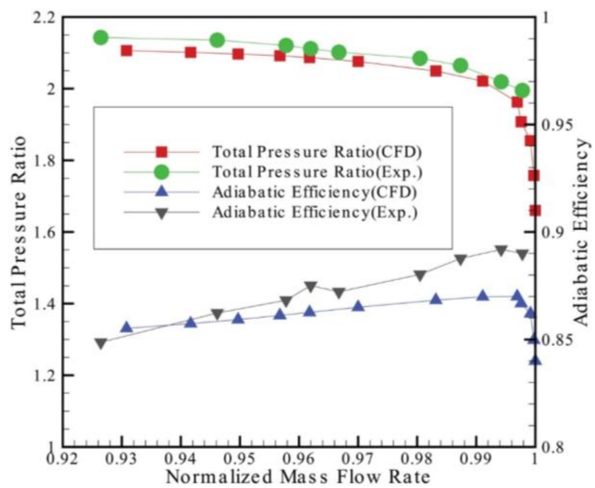

Fig. 5 Experimental and Numerical performance map of NASA Rotor 37.

5 RESULTS AND DISCUSSIONS

Changing the static pressure at the outlet region of the rotor causes some changes in the inlet axial velocity of compressor and rotor pressure ratio. For each designed leaned rotor blade, the flow field has been simulated around the blade and the rotor characteristic map has been predicted for all pressure ratios.

According to each rotor characteristics map, Table 4 presents the first ninth high-peak efficiency leaned blade and radial stacking line blade (Original) with their corresponding pressure ratio (PReak). As seen in this table, in all new geometries, the value of θ4 is 3o. In addition, at this value of θ4, by changing the lean angle in other control points, the changes of ηPeak and PRPeak become nominal, showing that, there is no significant effect on the ηPeak and PRPeak. On the other hand, about the efficiency increment, leaning the blade in the outer part of the blade is more effective than the inner part of the blade.

© 2018 IAU, Majlesi Branch

Table 3 The geometrical characteristics of the high adiabatic efficiency leaned blades and original blade

Case No.	θ_1	θ_2	θ_3	θ_4	η_{Peak}	PR_{Peak}
16	0.5	1	1.8	3	89.41	1.356
38	0.5	0	0	3	89.41	1.355
8	0	0	0.4	3	89.40	1.355
9	0	0	0.2	3	89.40	1.355
18	-0.5	-0.85	0.4	3	89.39	1.355
3	0	0	0	3	89.39	1.355
40	-0.5	0	0	3	89.39	1.355
13	-0.5	0	0.4	3	89.38	1.355
17	-0.1	0.7	1.5	3	89.38	1.356
Original	0	0	0	0	88.86	1.346

The choking mass flow rate of different blades calculated by CFD, are presented in Fig. 6. The results show that, the maximum increment of choking mass flow rate was about 0.4% which is a negligible amount.

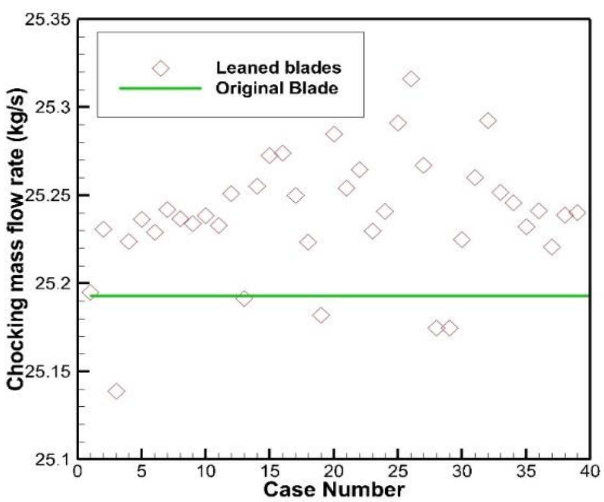

Fig. 6 Choking mass-flow rate of different leaned blades.

In comparison with all 40 designs, case 16 (Fig. 7) has a significant effect on the compressor rotor map. The lean angles of this blade at 0.25%, 50%, 75% and 100% of span are 0.5, 1.0, 1.8 and 3 degrees, respectively. The comparison of characteristics map between the proper leaned rotor and the original rotor is presented in Fig. 8.

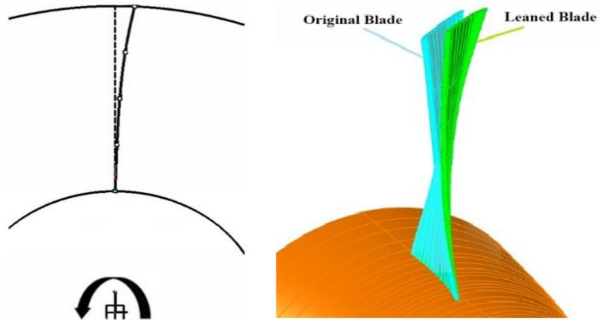

Fig. 7 Geometrical comparison of proper leaned blade and original blade..

The results show that, proper skewing stacking line of the blade in the tangential direction can increase the peak adiabatic efficiency from 88.86% to 89.41% (about 0.55% of increment). As it is seen, the total pressure ratio increases from 1.346 to 1.356 (nearly 0.75%).

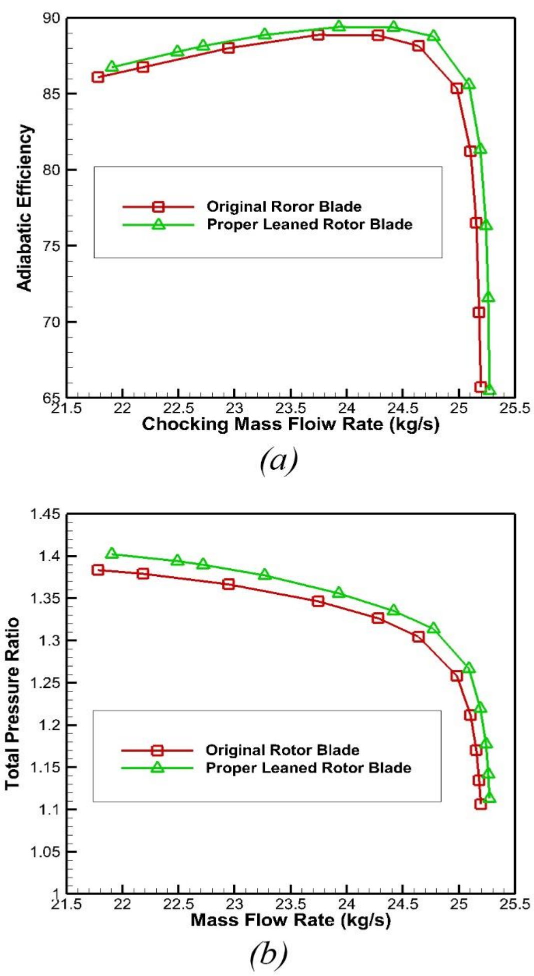

Fig. 8 The comparison of proper leaned blade and original blade characteristics map, (a): Adiabatic efficiency and (b): Total pressure ratio.

© 2018 IAU, Majlesi Branch

The radial distributions of performance quantities of proper leaned rotor and the original rotor at the peak efficiency condition in rotor outlet are compared in Fig. 9. Results show that, comparing to the original blade, in leaned blade, the total pressure ratio and the total temperature ratio are increased at the major part of the span. Also, the adiabatic efficiency increases in all parts of span, except near to the hub, however, there is no difference in the adiabatic efficiency at the shroud of both blades. Substantially, better performance is observed in leaned rotor blade.

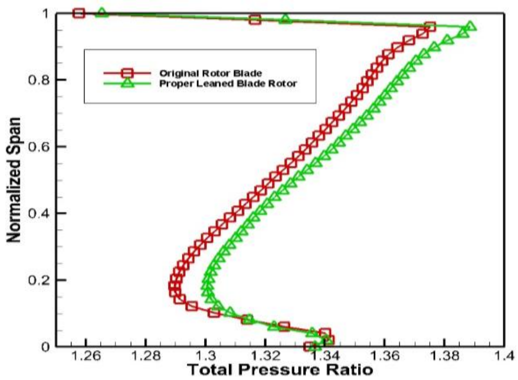

(a)

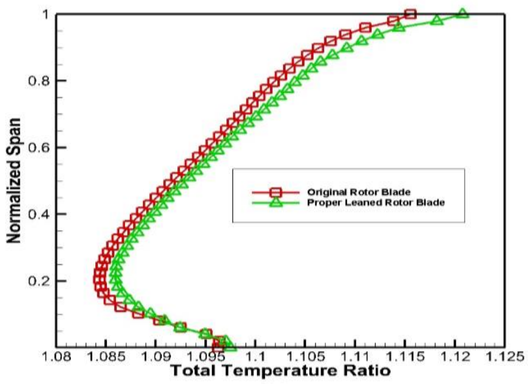

(b)

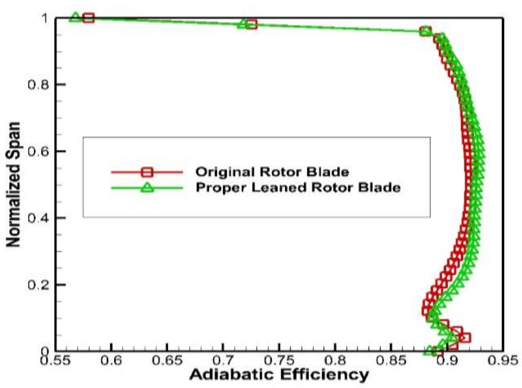

(c)

Fig. 9 Radial distributions of performance quantities at the peak efficiency condition, (a): Total pressure ratio, (b): Total temperature ratio and (c): Adiabatic Efficiency.

The suction surface streamlines for the original and leaned blades are compared in Fig. 10. The streamlines indicate that, comparing to the original blade, in leaned blade, both in the chord wise and the span wise directions, the secondary flow reduces and smaller part of the suction surface is exposed to the separation.

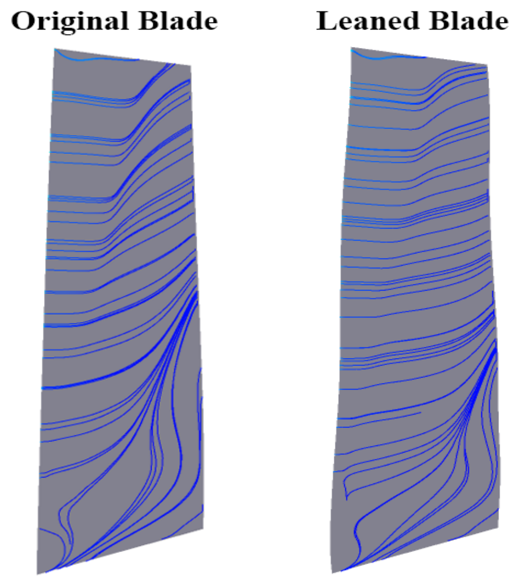

Fig. 10 Comparison of the suction surface streamlines in the original and leaned blades.

Figure 11 shows the static pressure contours on suction surfaces of original and leaned blades. The contours illustrate nearly similar shock wave pattern and location for both blades. However, for high aspect ratio rotor blade, leaning the blade has no effect on shock location

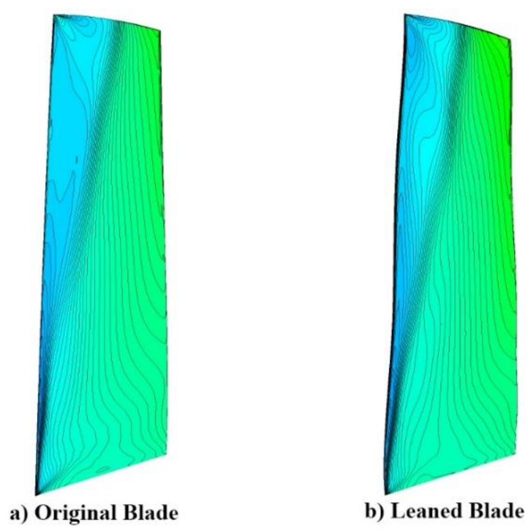

Fig. 11 Comparison of the suction surface pressure contours for original and leaned blades.

© 2018 IAU, Majlesi Branch

In peak efficiency condition and for the original and leaned blades, the relative Mach number distribution inside the blade passage is illustrated in Fig. 12 in 98%, 75% and 50% of span. Figure 12 indicates that, the shock pattern is similar to that of the original and leaned blades. However, in leaned blade, the shock intensity increases slightly.

Previous studies of high-transonic low-aspect-ratio rotor blades such as NASA Rotor 37 (AR=1.19, M_{tip}=1.48) indicated that, by leaning the blade, there are two major effects on the characteristics of rotor: First, reduction of the secondary flow and the second, movement of passage shock wave toward the downstream.

However, for low-transonic, high-aspect ratio rotor blade (AR=2.9, M_{tip}=1.2), the results demonstrate that, there is no significant movement of shock location by leaning the stacking line.

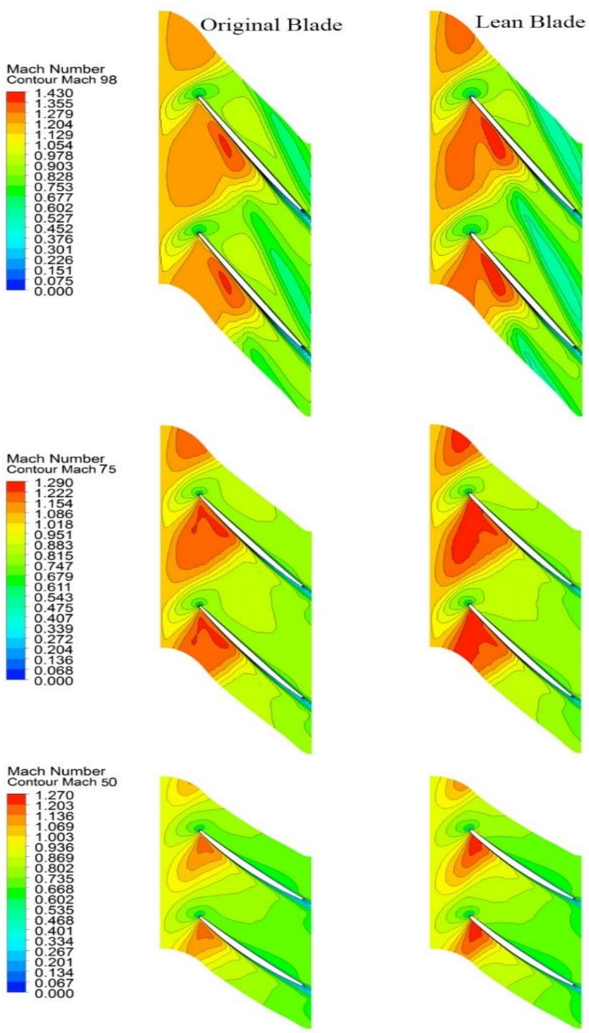

Fig. 12 Comparison of relative Mach-number distribution at 98%, 75% and 50% of span respectively in the original and leaned blades.

6 CONCLUSION

In present study, the effect of tangential change of stacking line on a high-aspect ratio transonic compressor rotor has been numerically investigated by a CFD code which solves the three-dimensional Reynolds-averaged Navier-Stokes equations. Too many blades with new stacking lines have been simulated. The results show that, the leaning of outer part of the blade is more effective than the inner part. By properly skewing the stacking line at four control points (0.25%, 50%, 75% and 100% of span), the adiabatic efficiency and total pressure ratio are increased up to 0.55% and 0.75%, respectively. In addition, the choking mass-flow increased about 0.4%. The results indicate that, lean angle at 100% span has most effect in the peak adiabatic efficiency rather than lean angle at other control points. The streamlines on the blade suction surface indicate that, the leaned blade causes the reduction of secondary flows and therefore, smaller part of span becomes exposed by the separation. But, the low-transonic, high-aspect ratio leaned blade has no effect on the shock wave location. By comparing the results of the current study with the studies of NASA Rotor 37, it can be implied that, leaning of the stacking line in high-transonic, low-aspect ratio rotor blade (AR=1.19, M_{tip}=1.48) causes the reduction of secondary flow and moves the shock wave location toward a blade rear, but in low-transonic, high-aspect ratio rotor blade (AR=2.9, M_{tip}=1.2) this issue only causes the reduction of secondary flow.

7 APPENDIX

Notation

Exp.	Experimental
LE	Leading Edge
M_{tip}	Rotor tip relative Mach number
PR_{Peak}	Pressure ratio at max efficiency
P_0	Total pressure
T_0	Total temperature
SST	Shear Stress Transport
y^+	Non-dimensional wall distance
η	Adiabatic efficiency
θ_1	Lean angle at 25% span
θ_2	Lean angle at 50% span
θ_3	Lean angle at 75% span
θ_4	Lean angle at 100% span

Abbreviations

ACM	Additive Correction Multigrid
CFD	Computational Fluid Dynamics
DCA	Double Circular Arc
IGV	Inlet Guide Vane
MCA	Multi Circular Arc

© 2018 IAU, Majlesi Branch

REFERENCES

[1] Weingold, H. D., Neubert, R. J., Behlke, R. F., et al., "Reduction of Compressor Stator Endwall Losses through the Use of Bowed Stators", Journal of Turbomachinery, Vol. 111, 1997, pp. 161- 168.

[2] Sasaki, T., Breugelmans, F., "Comparison of Sweep and Dihedral Effects on Compressor Cascade Performance", Journal of Turbomachinery, Vol. 120, 1998, pp. 454–463.

[3] Gummer, V., Wenger, U., and Kau, H. P., "Using Sweep and Dihedral to Control Three-Dimensional Flow in Transonic Stators of Axial Flow Compressor", Journal of Turbomachinery, Vol. 123, 2001, pp. 40-48.

[4] Gallimore, S. J., Bolger, J. J., Cumpsty, N. A., et al., "The Use of Sweep and Dihedral in Multistage Axial Flow Compressor Blading-Part II: Low and High-Speed Designs and Test Verification", Journal of Turbomachinery, Vol. 124, 2002, pp. 531-541.

[5] Gallimore, S. J., Bolger, J. J., Cumpsty, N. A., et al., "The Use of Sweep and Dihedral in Multistage Axial Flow Compressor Blading-Part I: University Research and Methods Development", Journal of Turbomachinery, Vol. 124, 2002, pp. 521–532.

[6] Roy, B., Laxmiprasanna, P. A., Borikar, V., et al., "Low Speed Studies of Sweep and Dihedral Effects on Compressor Cascades", Proceeding of ASME TURBO EXPO 2002, Amsterdam, Netherlands, Vol. 3-6, 2002, pp. GT-2002-30441.

[7] Bergner, J., Hennecke, D. K., Hoeger, M., et al., "Darmstadt Rotor No.2- Part II: Design of Lean Rotor Blades", International Journal of Rotating Machin, Vol. 9, 2003, pp. 385–391.

[8] Fischer, A., Riess, W., and Seume, J. R., "Performance of Strongly Bowed Stators in a Four-Stage High-Speed Compressor", Journal of Turbomachinery, Vol. 126, 2004, pp. 333-338.

[9] Ahn, C. S., Kim, K. Y., "Aerodynamic Design Optimization of a Compressor Rotor with Navier-Stockes Analysis", Proceedings of the Institution of Mechanical Engineers, Part A: Journal of Power and Energy, Vol. 217, 2003, pp. 179-183.

[10] Denton, J. D., Xu, L., "The Effects of Lean and Sweep on Transonic Fan Performance", Proceeding of ASME TURBO EXPO 2002, Amsterdam, Netherlands, Vol. 3-6, 2002, pp. GT-2002-30327.

[11] Oyama, A., Liou, M. S., and Obayashi, S. h., "High-Fidelity Swept and Leaned Rotor Blade Design Optimization using Evolutionary Algorithm", 16th AIAA Computational Fluid Dynamics Conference, Orlando, Florida, Vol. 23-26, 2003, pp. AIAA 2003-4091.

[12] Takahashi, Y., Hamatake, H., and Katoh, Y., "Experimental and Numerical Investigations of Endwall Flow in a Bowed Compressor Cascade", 41st AIAA/ASME/SAE/ASEE Joint Propulsion Conference & Exhibit, Tucson, Arizona, Vol. 10-13, 2005, pp. AIAA 2005-3638.

[13] Jang, Ch. M., Samad, A., and Kim, K. Y., "Optimal Design of Swept, Leaned and Skewed Blades in a Transonic Axial Compressor", Proceedings of GT2006 ASME Turbo Expo 2006: Power for Land Sea and Air, Barcelona, Spain, Vol. 8-11, 2006, pp. GT-2006-90384.

[14] Yang, L., Hua, O., and Zhao-Hui D., "Optimization Design and Experimental Study of Low-Pressure Axial Fan with Forward-Skewed Blades", International Journal of Rotating Machine, 2007, Article ID 85275.

[15] Zhang, Y. J., Chen, F., Guo-tai, F., et al., "Effect of Turning Angle on Flow Field Performance of Linear Bowed Stator in Compressor at Low Mach Number", Chinese Journal of Aeronautics, Vol. 19, No. 4, 2006, pp. 271-277.

[16] Benini, E., "Three-Dimensional Multi-Objective Design Optimization of a Transonic Compressor Rotor", AIAA Journal of Propulsion Power, Vol. 20, No. 3, 2004, pp. 559–65.

[17] Benini, E., Biollo, R., "Aerodynamics of Swept and Leaned Transonic Compressor-Rotors", Journal of Applied Energy, Vol. 84, 2007, pp. 1012–1027.

[18] Sun, P., Han, J., Zhong, J., et al., "Effects of Bowed Stators on a Transonic Fan with Distorted Inlet", Proceedings of ASME Turbo Expo 2008: Power for Land, Sea and Air, Berlin, Germany, Vol. 9-13, 2008, pp. GT-2008-50523.

[19] Chen, F., Li, Sh., Su, J., et al., "Experimental Study of Bowed-Twisted Stators in an Axial Transonic Fan Stage", Chinese Journal of Aeronautics, Vol. 22, 2009, pp. 364-37.

[20] Razavi, S. R., Boroomand, M., "Optimal Design and Aerodynamics Study of Leaned Transonic Axial Flow Fan Rotors", ASME 2014 International Mechanical Engineering Congress and Exposition, Montreal, Quebec, Canada, Vol. 14–20, 2014, pp. IMECE 2014-39796.

[21] Hutchinson, B. R., Raithby, G. D., "A Multigrid Method Based on Additive Correction Strategy", Journal of Numerical Heat Transfer, Vol. 9, No. 5, 1986, pp. 511–37.

[22] Launder, B. E., Spalding, D. B., "The Numerical Computation of Turbulent Flows", Journal of Computational Methods in Applied Mechanical Engineering, Vol. 3, 1974, pp. 269–289.

[23] Moore, R. D., Reid, L., "Performance of Single Stage Axial Flow Transonic Compressor with Rotor and Stator Aspect Ratios of 1.19 and 1.26, Respectively, and with Design Pressure Ratio of 2.05", NASA TP 1659, April 1980.

© 2018 IAU, Majlesi Branch